Journal of Chemical Health Risks

www.jchr.org

JCHR (2025) 15(6), 417-427 | ISSN:2251-6727

Comparison of Whole Body Diffusion Weighted MRI and PET CT in Detection of Malignant Tumours

Dr. Harini V.[1], Dr. Kalaichezhian M.[2], Dr. Murugan G.[3], Dr. Baskar A.[4]

[1]Post Graduate, Department of Radiodiagnosis, Sree Balaji Medical College and Hospital, Chromepet, Chennai 600044, India.

[2]Professor, Department of Radiodiagnosis, Sree Balaji Medical College and Hospital,

Chromepet, Chennai 600044, India.

[3]Professor and Head of the Department, Department of Radiodiagnosis, Sree Balaji Medical College and Hospital, Chromepet, Chennai 600044, India.

[4]Assistant Professor, Department of Radiodiagnosis, Sree Balaji Medical College and Hospital,

Chromepet, Chennai 600044, India.

Corresponding Author: Dr. Kalaichezhian M., Professor, Department of Radiodiagnosis, Sree Balaji Medical College and Hospital, Chromepet, Chennai 600044, India.

Received date: 15/09/2025, ***Revised Date: 16/10/2025*** ***Accepted Date: 06/11/2025***

Keywords:

PET CT, MRI, Malignant Tumours, Diagnostic Performance

ABSTRACT:

Background: Accurate whole-body assessment of malignancies is crucial for staging, treatment planning, and monitoring. Whole-body diffusion-weighted MRI (WB-DWI-MRI) and positron emission tomography-computed tomography (PET-CT) are increasingly utilized for this purpose, yet direct comparative data remain limited.

Objectives: This study aimed to compare the diagnostic performance of WB-DWI-MRI and PET-CT in detecting malignant lesions, evaluate their correlation with quantitative biomarkers—apparent diffusion coefficient (ADC) and standardized uptake value (SUV)—and characterize metastatic patterns across cancer types.

Methods: Nineteen patients with various histologically or radiologically diagnosed malignancies underwent both WB-DWI-MRI and PET-CT imaging. Detected lesions were analyzed for number, distribution, ADC, and SUV values. Diagnostic accuracy, sensitivity, specificity, positive predictive value (PPV), and negative predictive value (NPV) were calculated for each modality.

Results: Both WB-DWI-MRI and PET-CT showed high diagnostic performance. DWI-MRI achieved an overall sensitivity of 83.3%, specificity of 90%, PPV of 88.2%, and NPV of 85.7%, whereas PET-CT showed slightly higher values with a sensitivity of 88.9%, specificity of 95%, PPV of 94.7%, and NPV of 90.9%. A significant inverse correlation was observed between ADC and SUV values, indicating that lesions with lower ADC generally exhibited higher metabolic activity. Breast, thyroid, and gastrointestinal cancers showed the highest lesion burden, while thyroid cancers displayed more localized metastases.

Conclusion: PET-CT and WB-DWI-MRI are both highly effective for whole-body oncologic imaging. While PET-CT offers superior diagnostic accuracy, WB-DWI-MRI provides a radiation-free alternative suitable for younger or radiation-sensitive patients.Their complementary strengths support integrated use for improved tumor detection, staging, and follow-up in oncology practice.

INTRODUCTION

The accurate and timely identification of malignant tumors is crucial for improving clinical outcomes and tailoring appropriate therapeutic strategies in oncology[1,2]. Early detection and precise staging of cancers allow for better prognostication, informed treatment planning, and improved survival rates. Traditionally, oncological imaging has relied heavily on

Journal of Chemical Health Risks

www.jchr.org

JCHR (2025) 15(6), 417-427 | ISSN:2251-6727

anatomical and functional modalities, with Positron Emission Tomography–Computed Tomography (PET-CT) playing a pivotal role in tumor detection, staging, restaging, and treatment response monitoring[1,2]. PET-CT combines the functional capabilities of PET with the high-resolution anatomical detail provided by CT, offering a comprehensive view of tumor biology and burden within the body.

Over the past two decades, there has been growing interest in radiation-free imaging techniques that can provide comparable or superior diagnostic accuracy without the risks associated with ionizing radiation. Whole-body Magnetic Resonance Imaging (WB-MRI) has emerged as a powerful alternative in this context, particularly for systemic malignancy assessment[3,4]. This shift has been driven by technological advancements in MRI hardware, faster imaging sequences, and improved post-processing tools, which have significantly enhanced the quality and efficiency of whole-body imaging.

PET-CT functions by using radiotracers such as ^18F-fluorodeoxyglucose (FDG) that highlight areas of increased glucose metabolism, a hallmark of many malignancies. Cancer cells typically demonstrate enhanced glycolytic activity compared to normal tissues, resulting in increased FDG uptake and making PET-CT a highly sensitive method for tumor localization and metabolic characterization[1,2]. However, PET-CT has inherent limitations, including exposure to ionizing radiation, high operational costs, and potential false positives in inflammatory or infectious conditions.

In 2004, Takahara *et al.* introduced whole-body diffusion-weighted imaging with background body signal suppression (DWIBS), enabling functional imaging during free-breathing conditions and laying the foundation for the use of whole-body diffusion-weighted imaging (WB-DWI) in oncologic practice[5]. Diffusion-weighted imaging (DWI) exploits the Brownian motion of water molecules within tissues, which is often restricted in highly cellular environments such as malignant tumors. Because many tumors display both increased metabolic activity and restricted water diffusion, WB-DWI has shown potential as a functional imaging modality that can detect malignancies similar to PET imaging, without the use of ionizing radiation[6].

DW-MRI has therefore gained attention as a promising imaging technique for cancer detection and monitoring, offering the advantage of radiation-free imaging while providing functional information about tissue cellularity. The ability of DWI to highlight areas of restricted diffusion enables the differentiation of malignant tumors from normal tissue, contributing to improved lesion conspicuity and diagnostic confidence. Furthermore, WB-DWI enables comprehensive evaluation of the entire body in a single session, which is particularly useful for staging cancers that are known to metastasize widely[7].

Despite these advantages, one of the known limitations of WB-DWI is its relatively low spatial resolution, which can affect the visualization of detailed anatomical structures[8]. This limitation can lead to challenges in precisely localizing lesions, particularly when they are small or located adjacent to complex anatomy. To overcome this, WB-DWI is often combined with other MRI sequences that offer better anatomical detail. Similar to how the CT component of PET/CT enhances anatomical localization and diagnostic accuracy, combining WB-DWI with whole-body T2-weighted imaging (wbT2) may improve lesion detection and characterization by providing both functional and structural information[9]. Fat-suppressed whole-body T2-weighted imaging, commonly acquired using short tau inversion recovery (STIR) sequences, is frequently used alongside WB-DWI to enhance lesion conspicuity and provide high-quality anatomical context[10].

However, unlike PET/CT—which primarily detects functional and metabolic changes—MRI largely identifies structural or morphological alterations, limiting its capacity to capture early functional abnormalities before structural changes occur (11,12). This key difference underlines the complementary nature of the two modalities. While PET-CT excels at identifying metabolically active lesions even before anatomical changes are visible, WB-DWI MRI provides excellent soft tissue contrast and functional data without radiation, making it suitable for repeated follow-ups and pediatric or young adult populations[13].

Given these complementary strengths and limitations, a direct comparative evaluation of WB-DWI MRI and PET-CT in the detection of malignant tumors is essential to better understand their respective diagnostic roles. Such evidence could help optimize cancer imaging pathways, minimize radiation exposure, and improve patient outcomes. Through this comparative analysis, the study seeks to contribute valuable insights that can refine cancer imaging protocols and inform clinical decision-making in oncology[14]. This study, therefore, aims to evaluate and compare the imaging performance of WB-DWI MRI and PET-CT in detecting malignant tumors and to assess the distribution of metastases.

METHODOLOGY

Study Design

This was a hospital-based cross-sectional observational study designed to compare the diagnostic performance of

Journal of Chemical Health Risks

www.jchr.org

JCHR (2025) 15(6), 417-427 | ISSN:2251-6727

whole-body diffusion-weighted magnetic resonance imaging (WB-DWI MRI) and positron emission tomography–computed tomography (PET-CT) in detecting malignant tumors. The study involved a single-time-point assessment of each participant using both imaging modalities. Findings from the two modalities were compared for lesion detection and distribution analysis.

Study Setting

The study was conducted at two tertiary care institutions in Chennai, Tamil Nadu, India. WB-DWI MRI was performed at the Department of Radiodiagnosis and Imaging, Sree Balaji Medical College and Hospital, while PET-CT imaging was carried out at the Department of Nuclear Medicine, Dr. Rela Institute and Medical Centre. Both centers are well-equipped with advanced imaging facilities and cater to a high volume of oncological cases, making them ideal for conducting this comparative imaging study.

Study Period

The study was conducted over an 18-month period, spanning from January 2023 to January 2025. This period allowed for adequate recruitment of participants and completion of imaging, data collection, and preliminary analysis.

Study Population

The study population included adult patients aged between 18 and 70 years with a confirmed diagnosis of malignancy or strong clinical suspicion of malignant lesions. A total of 19 participants (both male and female) were enrolled. The inclusion of patients with varying tumor types and sites provided a diverse sample for evaluating the diagnostic capability of both imaging modalities across different malignancies.

Inclusion Criteria

Participants were eligible if they met the following criteria:

- Adults aged between 18 and 70 years.
- Patients with pathologically confirmed malignancy or strong radiological suspicion of malignant lesions.
- Patients with either focal or widespread malignant involvement.
- Individuals who provided written informed consent to participate in the study.

Exclusion Criteria

Participants were excluded from the study based on the following criteria:

- Contraindications to MRI such as cardiac pacemakers, metallic implants, or other non-MRI-compatible devices.
- Claustrophobia or inability to tolerate MRI examination.
- Presence of silicone breast implants (due to imaging artifacts).
- Refusal or inability to provide written informed consent.

Sample Size and Sampling Technique

The sample size was calculated based on findings from a previous study by Maccioni *et al.* (2023) (13), which reported a correlation coefficient of 0.65 between diffusion-weighted MRI and PET CT parameters. Considering a desired statistical power of 80% and a 95% confidence level, the minimum required sample size was estimated to be 19 participants. A non-probability convenience sampling technique was employed, considering the specific inclusion criteria and the feasibility of recruiting participants within the given study period.

Data Collection Procedure

Patients fulfilling the inclusion criteria were identified during their routine clinical evaluation at the participating departments. After initial screening, eligible participants were approached and informed about the study objectives, procedures, and voluntary nature of participation. Those who provided written informed consent were enrolled.

Demographic details, including age, sex, and type of malignancy, were documented. Relevant clinical history, including comorbidities such as diabetes mellitus, hypertension, cardiovascular disease, and respiratory conditions, was also recorded.

Each participant underwent both WB-DWI MRI and PET-CT imaging within a short interval to ensure comparability. The imaging studies were performed as follows:

Whole-Body Diffusion-Weighted MRI Protocol

WB-DWI MRI scans were performed on a 3.0 Tesla Siemens MRI scanner. Participants were positioned supine and feet-first on the scanner table. A Q-body coil was used for both signal transmission and reception. The imaging was performed using a matrix-based whole-

Journal of Chemical Health Risks

www.jchr.org

JCHR (2025) 15(6), 417-427 | ISSN:2251-6727

body acquisition protocol with automated table movement.

The scan covered the entire body from the skull base to the feet, divided into multiple overlapping stacks (typically 7–8 stacks depending on the participant's height). Each stack captured a specific body region, including the head and neck, thorax, abdomen, pelvis, thighs, knees, and calves. Diffusion-weighted images were acquired using free-breathing echo-planar imaging sequences with multiple b-values, and background body signal suppression was applied (DWIBS technique). Apparent diffusion coefficient (ADC) maps were automatically generated on the scanner console for quantitative analysis of lesion diffusion characteristics.

PET-CT Imaging Protocol

Whole-body PET-CT scans were performed using a 16 mm slice PET-CT scanner at Dr. Rela Institute and Medical Centre. Patients were instructed to fast for at least six hours before the procedure. Approximately 60 minutes after intravenous administration of ^18F-fluorodeoxyglucose (FDG), whole-body imaging was performed from the skull base to the mid-thigh level, and extended to the lower limbs where clinically indicated.

The PET component provided functional information by detecting areas of increased FDG uptake, while the CT component provided anatomical localization and attenuation correction. Images were reconstructed and interpreted on a dedicated workstation. Standardized uptake values (SUV) were calculated for each lesion to quantify metabolic activity.

Data Processing and Comparative Evaluation

For each participant, the number, anatomical location, and size of lesions detected on WB-DWI MRI and PET-CT were recorded and compared. ADC values (from MRI) and SUV values (from PET-CT) were documented for each lesion, enabling a side-by-side evaluation of functional characteristics. Lesions were categorized as present or absent on each modality, and concordance or discordance between the two imaging techniques was noted. This allowed for assessment of the sensitivity and specificity of WB-DWI relative to PET-CT, which was considered the reference standard.

Ethical Considerations

Ethical clearance for the study was obtained from the Institutional Human Ethics Committee of Sree Balaji Medical College and Hospital, Chennai, under approval number 002/SBMCH/IHEC/2023/1954. All participants provided written informed consent before enrolment. Confidentiality of all participant data was strictly maintained, and identifying information was anonymised before analysis. Participants were informed that their decision to participate or withdraw would not affect their clinical care in any way.

Statistical Analysis

All data were entered in Microsoft Excel and analyzed using IBM SPSS Statistics software (version 26). Continuous variables, such as age, ADC, and SUV values, were expressed as mean ± standard deviation (SD). Categorical variables, such as gender and lesion presence, were summarized as frequencies and percentages. Association between normally distributed continuous variables were done by independent samples t test.The diagnostic performance of WB-DWI MRI relative to PET-CT was assessed by calculating sensitivity, specificity, positive predictive value (PPV), negative predictive value (NPV), and overall accuracy. A p-value <0.05 was considered statistically significant.

RESULTS

A total of 19 patients were included in the study, comprising 11 males (57.9%) and 8 females (42.1%), with a mean age of 54.84 ± 6.53 years. The primary lesions identified were thyroid in 4 patients (21.1%), lung in 3 (15.8%), breast in 3 (15.8%), colorectal in 2 (10.5%), stomach in 2 (10.5%), and one each involving the pancreas (5.3%), ovary (5.3%), kidney (5.3%), prostate (5.3%), and lymphoma of the neck (5.3%). The method of diagnosis was radiological evaluation in 12 patients (63.2%) and biopsy confirmation in 7 patients (36.8%). (Table 1)

Table 1: Combined Demographic and Diagnostic Summary Table (n=19)

Variable	**Categories/Values**	**Count (n)**	**Percentage (%)**
Gender	Male	11	57.9
	Female	8	42.1
Age (**Mean ± SD**)	54.84 ± 6.534		
	Thyroid	4	21.1

Journal of Chemical Health Risks

www.jchr.org

JCHR (2025) 15(6), 417-427 | ISSN:2251-6727

Types of Primary Lesion	Lung	3	15.8
	Breast	3	15.8
	Colorectal	2	10.5
	Stomach	2	10.5
	Pancreatic	1	5.3
	Ovarian	1	5.3
	Kidney	1	5.3
	Prostate	1	5.3
	Lymphoma (Neck)	1	5.3
Diagnostic Method Used	Radiological	12	63.2
	Biopsy	7	36.8

Across the 19 patients studied, a total of 55 metastatic lesions were detected as shown in Table 2. Metastases were detected in multiple organs, most commonly "the lungs, liver, lymph nodes, bones, brain, and peritoneum". Lesion counts varied per individual, ranging from a single lesion to as many as five, culminating in a total of 55 lesions across the study group. Breast and ovarian cancers exhibited widespread metastases, frequently affecting four or more anatomical sites, whereas malignancies such as pancreatic and prostate cancers showed fewer, yet clinically significant, metastatic deposits.

Table 2: Types of primary lesion, metastasis and Number of lesions detected Distribution among all the study participants

Type of primary lesion	**Metastasis**	**No. of metastatic lesions detected**
Lung	Lymph nodes, liver, bones, brain	4
Thyroid	Lungs	1
Stomach	Peritoneum, liver, lungs	3
Colorectal	Lungs, liver	2
Breast	Lymph nodes, lungs, liver, bones	4
Lung	brain	1
Pancreatic	Liver, peritoneum	2
Colorectal	Lungs, liver, lymph nodes	3
Stomach	Peritoneum, liver, lungs, bone	4
Kidney	Lungs, liver, lymph nodes	3
Lung	Lymph nodes, liver	2
Thyroid	Lungs, liver	2
Prostate	Bones, lymph nodes, liver	3
Ovarian	liver, lungs, lymph nodes, Peritoneum	4
Breast	brain, lungs, liver, bones	4

Journal of Chemical Health Risks

www.jchr.org

JCHR (2025) 15(6), 417-427 | ISSN:2251-6727

Thyroid	Lungs, bones, liver	3
Breast	Lymph nodes, liver, bones	3
Lymphoma (Neck)	lymph node, Liver, Lung, Spleen, bone	5
Thyroid	Lungs, liver	2
Total	55	

Figure 1 shows the distribution of primary lesions to 55 metastatic lesions among the 19 patients included in the study. Thyroid carcinoma (4 patients) and lung carcinoma (3 patients) together accounted for 15 lesions (8 and 7 lesions, respectively), while breast carcinoma (3 patients) contributed 11 lesions. Colorectal and stomach carcinomas (2 patients each) together accounted for 12 lesions (5 from colorectal and 7 from stomach). Pancreatic, ovarian, kidney, and prostate carcinomas (1 patient each) collectively contributed 12 lesions (2, 4, 3, and 3 lesions, respectively). Additionally, one patient with lymphoma of the neck had 5 lesions.

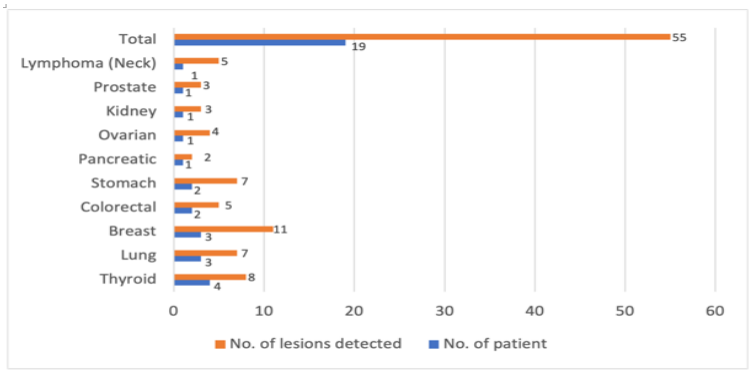

Figure 1: Distribution of primary lesions to metastatic lesions among the study participants (n=19)

Table 3 summarizes the ADC and SUV for all participants detailing both primary and metastatic lesion metrics detected by whole-body DWI MRI (ADC values) and PET CT (SUV values). ADC values for primary tumors ranged from 0.7 to 1.5 × 10^{-3} mm^2/s, while SUVmax values varied from 3.9 to 10, reflecting diverse tumor characteristics and cellularity, with low ADC and high SUV generally indicating aggressive, hypercellular tumors such as pancreatic and stomach cancers. Metastatic involvement spanned multiple anatomical sites including lymph nodes, liver, lungs, bones, brain, peritoneum, and spleen, consistently showing lymph nodes and liver as sites of restricted diffusion (ADC ~1.0–1.1) and elevated metabolic activity (SUV ~8–10). Overall, the dataset reveals a statistically significant inverse relationship between ADC and SUV values (mean ADC 1.14, SD 0.227; mean SUV 6.36, SD 1.84, $p = 0.001$) by independent samples t test, underscoring the complementary roles of MRI and PET CT in tumor evaluation and metastatic staging.

Table 3: Distribution of ADC and SUV Metrics for Primary and Metastatic Lesions

S.No	Primary Tumor	Primary ADC (10^{-3} mm^2/s)	Primary SUVmax	Metastasis Site(s)	Metastasis ADC (10^{-3} mm^2/s)	Metastasis SUV
1	Lung	1.1	4.0	Lymph nodes, Liver, Bones, Brain	1.1, 1.2, 0.8, 0.9	9.8, 7.6, 4.2, 6.8
2	Thyroid	1.3	3.9	Lungs	1.2	5.3
3	Stomach	0.7	6.9	Peritoneum, Liver, Lungs	0.9, 1.0, 1.2	6.2, 8.0, 5.0
4	Colorectal	1.0	5.8	Lungs, Liver	1.1, 1.0	5.1, 7.8

Journal of Chemical Health Risks

www.jchr.org

JCHR (2025) 15(6), 417-427 | ISSN:2251-6727

5	Breast	1.5	6.1	Lymph nodes, Lungs, Liver, Bones	1.1, 1.1, 1.0, 0.8	10.1, 5.2, 8.1, 4.5
6	Lung	1.2	4.1	Brain	0.9	7.5
7	Pancreatic	0.9	9.4	Liver, Peritoneum	1.0, 0.9	8.1, 6.4
8	Colorectal	1.2	6.2	Lungs, Liver, Lymph nodes	1.2, 1.0, 1.1	5.3, 8.0, 10.3
9	Stomach	0.8	7.3	Peritoneum, Liver, Lungs, Bone	0.8, 1.0, 1.1, 0.8	6.1, 8.2, 5.4, 4.3
10	Kidney	1.1	4.3	Lungs, Liver, Lymph nodes	1.2, 1.0, 1.1	5.5, 8.5, 10.5
11	Lung	1.5	4.6	Lymph nodes, Liver	1.1, 1.0	9.9, 7.9
12	Thyroid	0.9	8.3	Lungs, Liver	1.1, 1.0	5.2, 7.6
13	Prostate	1.2	7.1	Bones, Lymph nodes, Liver	0.8, 1.1, 1.0	4.1, 10.2, 8.0
14	Ovarian	1.1	5.4	Liver, Lungs, Lymph nodes, Peritoneum	1.0, 1.1, 1.1, 0.9	8.2, 5.6, 10.1, 6.0
15	Breast	1.2	5.6	Brain, Lungs, Liver, Bones	0.9, 1.1, 1.0, 1.8	7.3, 5.4, 7.9, 4.2
16	Thyroid	1.0	7.8	Lungs, Bones, Liver	1.1, 0.8, 1.0	5.2, 4.3, 8.1
17	Breast	1.3	5.7	Lymph nodes, Liver, Bones	1.1, 1.0, 0.8	10.4, 7.8, 4.4
18	Lymphoma (Neck)	1.5	10.0	Lymph node, Liver, Lung, Spleen, Bone	1.0, 1.0, 1.1, 0.8, 0.8	10.3, 7.8, 5.5, 6.2, 4.3
19	Thyroid	1.2	8.5	Lungs, Liver	1.1, 1.0	5.4, 8.0

Table 4 presents the comparative sensitivity and specificity of DWI MRI (ADC values) and PET CT (SUV values) for detecting metastatic lesions across different organs. PET CT demonstrated consistently higher sensitivity and specificity than DWI MRI in most sites, particularly for lymph nodes (95.3% and 91.4% vs. 89.5% and 86.2%), bones (94.7% and 90.1% vs. 90.2% and 87.9%), lungs (92.5% and 89.3% vs. 83.4% and 81.2%), and peritoneum (90.1% and 88.5% vs. 86.3% and 84.2%). In the liver, both modalities showed comparable performance, with DWI MRI achieving 92.7% sensitivity and 90.5% specificity, while PET CT showed 93.8% and 88.9%, respectively. Interestingly, DWI MRI outperformed PET CT in detecting brain metastases, demonstrating higher sensitivity (88.6% vs. 78.9%) and specificity (88.1% vs. 74.6%). For splenic lesions, PET CT also showed slightly better diagnostic accuracy (91.7% and 89.3% vs. 88.1% and 85.6%). Overall, PET CT exhibited superior diagnostic accuracy across most anatomical sites, except for brain metastases, where DWI MRI performed better.

Table 4: "Sensitivity and specificity of DWI MRI and PET CT for detecting metastatic lesions among the study participants"

Type of lesions	Modality	Sensitivity	Specificity
Lymph Nodes	DWI MRI (ADC)	89.5	86.2
	PET CT (SUV)	95.3	91.4

Journal of Chemical Health Risks

www.jchr.org

JCHR (2025) 15(6), 417-427 | ISSN:2251-6727

Liver	DWI MRI (ADC)	92.7	90.5
	PET CT (SUV)	93.8	88.9
Bones	DWI MRI (ADC)	90.2	87.9
	PET CT (SUV)	94.7	90.1
Brain	DWI MRI (ADC)	88.6	88.1
	PET CT (SUV)	78.9	74.6
Lungs	DWI MRI (ADC)	83.4	81.2
	PET CT (SUV)	92.5	89.3
Peritoneum	DWI MRI (ADC)	86.3	84.2
	PET CT (SUV)	90.1	88.5
Spleen	DWI MRI (ADC)	88.1	85.6
	PET CT (SUV)	91.7	89.3

Table 5 presents a comparison of the diagnostic accuracy of DWI MRI and PET CT based on sensitivity, specificity, PPV, and NPV among the participants. PET CT outperformed DWI MRI with a higher sensitivity (88.89% vs. 83.33%) and specificity (95% vs. 90%). Similarly, PET CT showed slightly higher PPV (94.74% vs. 88.24%) and NPV (90.91% vs. 85.71%) than DWI MRI, suggesting better overall diagnostic performance.

Table 5: Diagnostic Performance of DWI MRI and PET CT among the Study Participants

Parameter	DWI MRI (%)	95% CI	PET CT (%)	95% CI
Sensitivity	83.33	62.6 – 95.3	88.89	70.8 – 97.6
Specificity	90.00	68.3 – 98.8	95.00	75.1 – 99.9
PPV	88.24	65.7 – 96.7	94.74	73.9 – 99.1
NPV	85.71	63.7 – 95.5	90.91	69.3 – 98.4

DISCUSSION

In this study, there was a slight male predominance, with men comprising 57.9% and women 42.1%. This aligns with Evangelista *et al.* (2013), who observed greater male representation in imaging-based oncology studies, particularly in lung and colorectal cancers[16]. Conversely, Gabrielle Mayer *et al.* (2025) reported female-majority cohorts in breast and gynecological cancer studies, highlighting how tumor type shapes gender distribution[17].

The mean age was 54.84 years, comparable to prior studies on advanced oncologic imaging. Arslan *et al.* (2020) reported a mean age of 59 years among patients undergoing PET-CT, particularly for breast and colorectal cancers[18]. Padhani *et al.* (2011) also noted that whole-body diffusion-weighted MRI (WB-DWI-MRI) is commonly performed in the fifth and sixth decades[19]. In contrast, Liu *et al.* (2022) observed a younger mean age (45 years) in a cohort dominated by gynecological and thyroid cancers, showing that malignancy type shapes the age profile[20].

Thyroid carcinoma was the most frequent primary tumor (21.1%), followed by lung and breast cancers (15.8% each). This differs from earlier studies where lung and breast were predominant. Shankar *et al.* (2006) reported lung as the leading malignancy in PET-CT and DW-MRI cohorts[21], and Mehrotra *et al.* (2022) found breast cancer most prevalent in women undergoing whole-body imaging[22]. The higher proportion of thyroid cancers here parallels Panato *et al.* (2020), who observed a rising trend in thyroid malignancies in India, especially among middle-aged women[23]. Such differences reflect regional cancer epidemiology and referral patterns.

Journal of Chemical Health Risks

www.jchr.org

JCHR (2025) 15(6), 417-427 | ISSN:2251-6727

Radiology identified 63.2% of malignancies, while 36.8% were biopsy-confirmed. This reflects the growing reliance on imaging in cancer diagnosis. Ming *et al.* (2020) emphasized PET-CT and DWI-MRI's role when biopsy is infeasible or risky[24]. In contrast, Connal *et al.* (2023) reported biopsy as the primary diagnostic modality in over 70% of cases, reaffirming its role as the gold standard[25]. This study illustrates how imaging complements histopathology in whole-body evaluation.

Breast and ovarian cancers showed the highest metastatic burden, with up to four metastatic sites per patient. Lung, stomach, and colorectal cancers also exhibited substantial spread. Koh *et al.* (2007) similarly noted that breast and gastrointestinal malignancies frequently metastasize to multiple organs, especially liver and bones, as seen on WB-DWI-MRI and PET-CT[13]. Combes *et al.* (2022) also highlighted PET-CT's high sensitivity for multi-organ metastases, especially in lung and prostate cancers[26]. Thus, metastatic patterns reflect both tumor biology and population factors.

Overall, 55 metastatic lesions were identified among 19 patients. Breast cancer contributed the highest lesion count (11 lesions across 3 patients), followed by thyroid (8) and stomach (7). This aligns with Messiou *et al.* (2021), who reported high lesion burden in breast and gastrointestinal cancers[27]. Multiple lesions in lung and colorectal cancers mirror Kim *et al.* (2023), who described frequent multifocal disease[28]. In contrast, Nakanishi *et al.* (2020) reported fewer lesions in thyroid and prostate cancers, suggesting that the higher counts here may reflect more aggressive variants or later-stage disease[29]. The detection of five lesions in a lymphoma case aligns with Quintanilla-Martinez *et al.* (2023), who described its multifocal nature[30]. These patterns emphasize the heterogeneity of metastatic behavior and the value of whole-body imaging for staging.

Quantitative analysis showed ADC values ranging from 0.7 to 1.5 × 10^{-3} mm^2/s and SUV values from 3.9 to 10. An inverse correlation was noted—lesions with lower ADC tended to have higher SUV, indicating higher cellular density and metabolic activity. Maman *et al.* (2020) similarly reported low ADC (0.7–0.9) and high SUV (6.9–9.4) in aggressive pancreatic and gastric cancers[31]. However, breast cancer and lymphoma lesions showed relatively higher ADC with high SUV, aligning with Koh *et al.* (2007), who noted that the inverse ADC-SUV relationship may not apply in tumors with heterogeneous cellular architecture (13). These findings highlight the complementary biological insights provided by DWI-MRI (cellularity via ADC) and PET-CT (metabolic activity via SUV).

The mean ADC was 1.14 × 10^{-3} mm^2/s (SD 0.2269), and mean SUV was 6.36 (SD 1.8415), with a statistically significant inverse correlation, confirming that lower ADC lesions were more metabolically active. Brandmaier *et al.* (2015) similarly demonstrated the combined utility of ADC and SUV in tumor characterization[32].

Regarding diagnostic performance, PET-CT showed higher sensitivity (88.89%) and specificity (95%) than DWI-MRI (83.33% and 90%). This agrees with Rama *et al.* (2022), who reported superior diagnostic accuracy of PET-CT for metastatic detection[33]. However, the strong performance of DWI-MRI is notable and supports Koh *et al.* (2007), who advocated its use as a non-invasive, radiation-free alternative[13]. The comparable efficacy suggests these modalities are complementary: PET-CT can serve as the reference for initial staging and metabolic profiling, while DWI-MRI may be preferred for follow-up, especially in younger or radiation-sensitive patients.

This study has few limitations. The overrepresentation of certain cancers, such as thyroid and breast malignancies, may have influenced the observed lesion distribution and diagnostic performance outcomes. Not all lesions were confirmed histologically, which could introduce diagnostic uncertainty. Additionally, potential inter-observer variability and the absence of standardized imaging intervals may have affected the accuracy of modality comparisons. Furthermore, cost-effectiveness, patient comfort, and long-term prognostic outcomes were not assessed, limiting the generalizability of the findings.

Despite these limitations, this study highlights the valuable complementary roles of DWI-MRI and PET-CT in whole-body oncologic imaging. PET-CT offers superior sensitivity and specificity, making it the preferred modality for initial staging, while DWI-MRI provides a radiation-free alternative well suited for follow-up, particularly in younger patients. The inverse correlation observed between ADC and SUV underscores the potential of combining functional and metabolic imaging to improve tumor characterization. Future multicenter studies with larger, more diverse cohorts and standardized imaging protocols are warranted to validate these findings and to optimize imaging strategies for comprehensive cancer evaluation.

CONCLUSION

The present study provides a comprehensive comparison of WB-DWI-MRI and PET-CT in detecting malignant tumors. Both modalities demonstrated high diagnostic performance, with PET-CT showing slightly superior

Journal of Chemical Health Risks

www.jchr.org

JCHR (2025) 15(6), 417-427 | ISSN:2251-6727

accuracy, while DWI-MRI offered the advantage of being radiation-free. The complementary use of ADC and SUV metrics highlighted their synergistic value in characterizing tumor biology. The study also revealed varying lesion burdens and metastatic patterns across malignancies, with breast, thyroid, and gastrointestinal cancers exhibiting a higher metastatic load. Although PET-CT showed an edge in diagnostic capability, the non-ionizing nature of DWI-MRI makes it particularly valuable for radiation-sensitive populations and for longitudinal follow-up. Overall, the findings support the integrated use of both imaging modalities to enhance detection, guide treatment planning, and monitor disease progression in oncology practice.

REFERENCES

1. Bar-Shalom R, Yefremov N, Guralnik L *et al.* Clinical performance of PET/CT in evaluation of cancer: additional value for diagnostic imaging and patient management. J Nucl Med . 2003; 44:1200–1209
2. von Schulthess GK, Steinert HC, Hany TF. Integrated PET/CT: current applications and future directions. Radiology. 2006; 238:405–422.
3. Kavanagh E, Smith C, Eustace S. Whole-body turbo STIR MR imaging: controversies and avenues for development. Eur Radiol. 2003; 13:2196–2205.
4. Hargaden G, O'Connell M, Kavanagh E, Powell T, Ward R, Eustace S. Current concepts in whole-body imaging using turbo short tau inversion recovery MR imaging. AJR Am J Roentgenol. 2003; 180:247–252
5. Takahara T, Imai Y, Yamashita T, Yasuda S, Nasu S, Van Cauteren M. Diffusion weighted whole body imaging with background body signal suppression (DWIBS): technical improvement using free breathing, STIR and high-resolution 3D display. Radiat. 2004; Med 22:275–282
6. Koh DM, Collins DJ. Diffusion-weighted MRI in the body: applications and challenges in oncology. AJR Am J Roentgenol 2007; 188:1622–1635.
7. Johnston C, Brennan S, Ford S, Eustace S. Whole body MR imaging: applications in oncology. Eur J Surg Oncol. 2006; 32:239– 246.
8. Albano D, Micci G, Patti C, Midiri F, Albano S, Lo Re G, Galia M. Whole-body magnetic resonance imaging: current role in patients with lymphoma. Diagnostics. 2021; 11(6):1007
9. Naganawa S, Kawai H, Fukatsu H *et al.* Diffusion-weighted imaging of the liver: technical challenges and prospects for the future. Magn Reson Med Sci. 2005; 4:175–186
10. Hany TF, Steinert HC, Goerres GW, Buck A, von Schulthess GK. Improvement of diagnostic accuracy of PET imaging using an in-line PET-CT system: preliminary results. J Nucl Med. 2002; 43:307p–307p
11. Schmidt GP, Reiser MF, Baur-Melnyk A. Whole-body MRI for the staging and follow-up of patients with metastasis. Eur J Radiol. 2009; 70:393–400.
12. Kwee TC, Takahara T, Ochiai R *et al.* Whole-body diffusion-weighted magnetic resonance imaging. Eur J Radiol. 2009; 70:409–417.
13. Koh DM, Takahara T, Imai Y, Collins DJ. Practical aspects of assessing tumors using clinical diffusion-weighted imaging in the body. Magn Reson Med Sci. 2007; 6:211–224
14. Kloth JK, Hillengass J, Listl K, Kilk K, Hielscher T, Landgren O, *et al.* Appearance of monoclonal plasma cell diseases in whole-body magnetic resonance imaging and correlation with parameters of disease activity. Int J Cancer 2014; 135: 2380–6.
15. Maccioni F, Alfieri G, Assanto GM, Mattone M, Gentiloni Silveri G, Viola F, De Maio A, Frantellizzi V, Di Rocco A, De Vincentis G, Pulsoni A, Martelli M, Catalano C. Whole body MRI with Diffusion Weighted Imaging versus 18F-fluorodeoxyglucose-PET/CT in the staging of lymphomas. Radiol Med. 2023 May;128(5):556-564.
16. Evangelista L, Zattoni F, Guttilla A, Saladini G, Zattoni F, Colletti PM, Rubello D. Choline PET or PET/CT and biochemical relapse of prostate cancer: a systematic review and meta-analysis. Clin Nucl Med. 2013 May;38(5):305-14.
17. Gabrielle Mayer *et al.* Breast and Gynecologic Cancer Care for Sexual Minority Women and Transgender People. Am Soc Clin Oncol Educ Book. 2025; 45 (3): e473608.
18. Arslan E, Aksoy T, Gürsu RU, Dursun N, Çakar E, Çermik TF. The Prognostic Value of ^{18}F-FDG PET/CT and KRAS Mutation in Colorectal Cancers. Mol Imaging Radionucl Ther. 2020 Feb 17;29(1):17-24.
19. Padhani, Anwar & Koh, Dow-Mu & Collins, David. Whole-Body Diffusion-weighted MR Imaging in Cancer: Current Status and Research Directions. Radiology. 2011; 261: 700-18.

Journal of Chemical Health Risks

www.jchr.org

JCHR (2025) 15(6), 417-427 | ISSN:2251-6727

20. Liu, Chunhao & Zhao, Hao & Xia, Yu & Cao, Yue & Zhang, Liyang & Zhao, Ya & Gao, Luying & Liu, Ruifeng & Liu, Yuewu & Liu, Hongfeng & Meng, Zhilan & Liu, Shuzhou & Li, Xiaoyi. Active surveillance of highly suspicious thyroid nodules cohort in China shows a worse psychological status in younger patients. Frontiers in Oncology. 2022; 12.

21. Shankar, L.K.; Hoffman, J.M.; Bacharach, S.; Graham, K.M.; Karp, J.; Lammertsma, A.A.; Larson, S.; Mankoff, D.A.; Siegel, B.A.; Abbeele, A.V.; *et al.* Consensus recommendations for the use of 18F-FDG PET as an indicator of therapeutic response in patients in National Cancer Institute Trials. J. Nucl. Med. 2006, 47, 1059–1066.

22. Mehrotra R, Yadav K. Breast cancer in India: Present scenario and the challenges ahead. World J Clin Oncol. 2022 Mar 24;13(3):209-218.

23. Panato C, Vaccarella S, Dal Maso L, Basu P, Franceschi S, Serraino D, Wang K, Lei F, Chen Q, Huang B, Mathew A. Thyroid Cancer Incidence in India Between 2006 and 2014 and Impact of Overdiagnosis. J Clin Endocrinol Metab. 2020 Aug 1;105(8):2507–14.

24. Ming Y, Wu N, Qian T, Li X, Wan DQ, Li C, Li Y, Wu Z, Wang X, Liu J, Wu N. Progress and Future Trends in PET/CT and PET/MRI Molecular Imaging Approaches for Breast Cancer. Front Oncol. 2020 Aug 12;10:1301.

25. Connal S, Cameron JM, Sala A, Brennan PM, Palmer DS, Palmer JD, Perlow H, Baker MJ. Liquid biopsies: the future of cancer early detection. J Transl Med. 2023 Feb 11;21(1):118.

26. Combes AD, Palma CA, Calopedos R, Wen L, Woo H, Fulham M, Leslie S. PSMA PET-CT in the Diagnosis and Staging of Prostate Cancer. Diagnostics (Basel). 2022 Oct 26;12(11):2594.

27. Messiou C, Porta N, Sharma B, Levine D, Koh DM, Boyd K, Pawlyn C, Riddell A, Downey K, Croft J, Morgan V, Stern S, Cheung B, Kyriakou C, Kaczmarek P, Winfield J, Blackledge M, Oyen WJG, Kaiser MF. Prospective Evaluation of Whole-Body MRI versus FDG PET/CT for Lesion Detection in Participants with Myeloma. Radiol Imaging Cancer. 2021 Sep;3(5):e210048.

28. Kim HJ, Sohn SY, Jang HW, Kim SW, Chung JH. Multifocality, but not bilaterality, is a predictor of disease recurrence/persistence of papillary thyroid carcinoma. World J Surg. 2013 Feb;37(2):376-84.

29. Nakanishi K, Tanaka J, Nakaya Y, Maeda N, Sakamoto A, Nakayama A, Satomura H, Sakai M, Konishi K, Yamamoto Y, Nagahara A, Nishimura K, Takenaka S, Tomiyama N. Whole-body MRI: detecting bone metastases from prostate cancer. Jpn J Radiol. 2022 Mar;40(3):229-244.

30. Quintanilla-Martinez L, Swerdlow SH, Tousseyn T, Barrionuevo C, Nakamura S, Jaffe ES. New concepts in EBV-associated B, T, and NK cell lymphoproliferative disorders. Virchows Arch. 2023 Jan;482(1):227-244.

31. Maman A, Sahin A, Ayan AK. The Relationship of SUV Value in PET-CT with Tumor Differentiation and Tumor Markers in Gastric Cancer. Eurasian J Med. 2020 Feb;52(1):67-72.

32. Brandmaier P, Purz S, Bremicker K, Höckel M, Barthel H, Kluge R, Kahn T, Sabri O, Stumpp P. Simultaneous [18F]FDG-PET/MRI: Correlation of Apparent Diffusion Coefficient (ADC) and Standardized Uptake Value (SUV) in Primary and Recurrent Cervical Cancer. PLoS One. 2015 Nov 9;10(11):e0141684.

33. Rama S, Suh CH, Kim KW, Durieux JC, Ramaiya NH, Tirumani SH. Comparative Performance of Whole-Body MRI and FDG PET/CT in Evaluation of Multiple Myeloma Treatment Response: Systematic Review and Meta-Analysis. AJR Am J Roentgenol. 2022 Apr;218(4):602-613.